Article

The Nitrate-Dependent Impact of Carbon Source Starvation on EH40 Steel Corrosion Induced by the Coexistence of *Desulfovibrio vulgaris* and *Pseudomonas aeruginosa*

Wenkai Wang [1,2,3,†], Zhihua Sun [1,2,3,4,†], Jiajia Wu [1,2,3,*], Dun Zhang [1,2,3,*], Peng Wang [1,2,3], Ce Li [1,2,3,4], Liyang Zhu [1,2,3,4], Yaohua Gao [1,2,3,4] and Yan Sun [1,2,3]

1   Key Laboratory of Marine Environmental Corrosion and Biofouling, Institute of Oceanology, Chinese Academy of Sciences, Qingdao 266071, China
2   Laoshan Laboratory, Qingdao 266237, China
3   Center for Ocean Mega-Science, Chinese Academic of Sciences, Qingdao 266071, China
4   University of Chinese Academy of Sciences, Beijing 100049, China
*   Correspondence: wujiajia@qdio.ac.cn (J.W.); zhangdun@qdio.ac.cn (D.Z.)
†   These authors contributed equally to this work.

Abstract: Carbon source starvation can promote steel corrosion in the presence of a pure culture through extracellular electron transfer (EET). However, the impact of carbon source starvation on corrosion induced by mixed strains is still unknown. This work investigated the impact of carbon source starvation on EH40 steel corrosion in the presence of *Desulfovibrio vulgaris* and *Pseudomonas aeruginosa*, typical species of sulfate- and nitrate-reducing bacteria. It was found that the impact of carbon source starvation on corrosion depended on nitrate addition. When nitrate (5 g·L^{-1} NaNO$_3$) was not added, the corrosion was promoted by carbon source starvation. However, the corrosion was initially promoted by carbon source starvation, but later inhibited with nitrate addition. The corrosion behaviors in different systems were closely related to different numbers of the strains in biofilms and their metabolic activities, and the mechanisms were revealed.

Keywords: microbiologically influenced corrosion; *Desulfovibrio vulgaris*; *Pseudomonas aeruginosa*; extracellular electron transfer; nitrate addition

1. Introduction

Microbiologically influenced corrosion (MIC) occurs universally in various environments. Initial reports on the possible acceleration of corrosion by bacteria date back to the late 19th and early 20th century [1,2]. However, the mechanisms of MIC are yet to be understood [3]. The extracellular electron transfer (EET) mechanism in MIC has attracted much attention in the past two decades. EET is commonly divided into mediated EET via extracellular electron shuttles and direct EET via conductive pilins and outer-surface *c*-type cytochromes [4–6]. Carbon source starvation is usually adopted to promote EET-MIC by forcing bacteria to obtain electrons from metals for energy generation [7,8]. Accelerated corrosion of metals under carbon source starvation is often conducted on pure cultures, such as *Pseudomonas aeruginosa*, *Desulfovibrio vulgaris*, *Natronorubrum tibetense*, and so on [7–9]. However, the effect of carbon source starvation on the corrosion response of metals and their alloys in the presence of mixed bacteria has not gained the same attention [10]. Practically, MIC is a result of consortia containing multiple strains. To the best of our knowledge, no reports exploring this topic are available.

Sulfate- (SRB) and nitrate-reducing bacteria (NRB) are well-known for their ability to accelerate MIC via EET. Much attention has been paid to the corrosion affected by their coexistence [11–16]. Fu et al. evaluated the corrosion behavior of X80 steel in the presence of SRB, NRB, and mixed biofilms in a soil solution containing 48 mg·L^{-1} sulfate

and 46 mg·L^{-1} nitrate. The corrosion rate of X80 steel was found to increase in the following order: sterile control < *Pseudomonas stutzeri* < *Desulfovibrio desulfurican* < co-cultures of *Desulfovibrio desulfurican* with *Pseudomonas stutzeri*, while the corrosivity of SRB was inhibited by the addition of NRB [17]. In contrast, the addition of *Thiomicrospira* sp. strain CVO, a typical nitrate-reducing bacteria, and 10 mM nitrate to *Desulfovibrio* sp. Lac6, a typical sulfate-reducing bacteria, increased the corrosion rate of carbon steel from 0.2 to 1.5 g·cm^{-2}·day^{-1} [15]. The differences in metals, bacterial strains, and environmental factors might be responsible for this conflict. The corrosion of a specific metal in the presence of specific mixed strains of SRB and NRB is dependent on environmental factors, among which the nitrate concentration is a rather significant factor. Nitrate regulates the activity of NRB and SRB, leading to different corrosion behaviors [18–20]. Recently, the influence of nitrate concentrations on steel corrosion in an organic-rich medium with the coexistence of *P. aeruginosa* (NRB) and *D. vulgaris* (SRB) has been investigated [21]. It was found that the corrosion rate increased with increasing nitrate concentrations from 0 to 5 g·L^{-1}, but decreased with further nitrate addition. The corrosion was positively correlated with the number of *P. aeruginosa* and their activity, which are controlled by nitrate [21]. Therefore, it is necessary to take the impact of nitrate on NRB and SRB into consideration in the study of corrosion affected by mixed cultures when carbon resource starvation is adopted.

In the present study, the impact of carbon source starvation on the corrosion of EH40 steel in the presence of mixed cultures, *D. vulgaris* and *P. aeruginosa*, was studied, and the role of nitrate was emphasized. The differences in corrosion behaviors in different systems were evaluated by weight loss, electrochemical measurements, and surface characterizations. The dependence of MIC affected by carbon source starvation on nitrate was revealed from the changes in quantity and activity of the strains.

2. Materials and Methods

2.1. Steel Specimen Preparation

The EH40 steel was purchased from Nanjing Iron & Steel Co., Ltd., (Nanjing, China). The chemical composition of the steel was as follows (wt.%): Al 0.034, C 0.086, Cr 0.118, Cu 0.028, Si 0.24, Mn 1.49, Mo 0.001, Nb 0.034, Ni 0.013, P 0.011, Ti 0.01, and Fe balance. EH40 steel was cut into coupons with dimensions of 5 mm × 5 mm × 3 mm, 10 mm × 10 mm × 5 mm, and 20 mm × 10 mm × 5 mm for different characterizations. The largest samples were for weight loss and surface analysis, except for X-ray photoelectron spectroscopy (XPS). Samples with dimensions of 10 mm × 10 mm × 5 mm were applied to prepare electrodes for electrochemical measurements, and those with the smallest size were for the XPS characterization.

To prevent crevice corrosion, the side faces of coupons were coated with polytetrafluoroethylene before electrochemical tests. The coated coupons were embedded with epoxy resin after being welded to copper wires (Shengli Chemical Technology Co., Ltd., Nanjing, China). For each working electrode, a face of 10 mm × 10 mm was exposed to media with and without bacteria. All coupons were polished, washed, dried, and sterilized according to previous reports [22].

2.2. Strains and Culture Condition

P. aeruginosa was incubated aerobically in 2216E medium and *D. vulgaris* was cultured anaerobically in a modified Postgate's medium, as previously reported [21]. The salinity of the natural seawater was 31.8‰. Filter sterilized L-cysteine was added to the medium to guarantee the anaerobic condition. Resazurin was added before sterilization as an anaerobic indicator.

Then, 4 mL pure cultures of *P. aeruginosa* and *D. vulgaris* at the exponential phase were transferred to the anaerobic Postgate's medium. After 3 days of pregrowth, biofilms formed on EH40 steel coupons. The coupons were then transported to anaerobic Postgate's medium with different modifications: the medium with full carbon source and without

nitrate addition, the medium without carbon source and nitrate addition, the medium with full carbon source and nitrate addition (5 g·L^{-1} NaNO$_3$), and the medium without carbon source and nitrate addition (5 g·L^{-1} NaNO$_3$).

2.3. Environmental Factor Measurements and Cell Counting

The pH values of the different media were measured by a pH meter (PHS-3C, Spectrum Test Equipment Technology Co., Ltd., Dongguan, China) after 14 days of incubation. The concentrations of HS$^-$, SO$_4^{2-}$, NO$_3^-$, and NO$_2^-$ in different systems were detected by ion chromatography.

The number of sessile cells was counted on the 7th and 14th days by the plate counting method after they were harvested from the surface of coupons and dispersed in sterile phosphate buffered saline (PBS) solution (Thermo Fisher Scientific Inc., Waltham, MA, USA). For *P. aeruginosa*, aerobic 2216E medium was chosen to preclude anaerobic *D. vulgaris*. For *D. vulgaris*, a modified medium was selected to distinguish *D. vulgaris* from *P. aeruginosa* by the specific HS$^-$ production, which consisted of yeast extract 1.00 g, tryptone 2.00 g, sodium lactate solution 2 mL, PIPES (1, 4-piperazine diethylsulfonate) 3.30 g, seawater 800 mL, distilled water 200 mL, and (NH$_4$)$_2$Fe(SO$_4$)$_2$·6H$_2$O 0.60 g. *D. vulgaris* catalyzed sulfate reduction to produce HS$^-$, which formed a black sediment with Fe^{2+}. Therefore, the colonies of *D. vulgaris* were black and those of *P. aeruginosa* were of their natural color.

2.4. Biofilm Observation

The coupons with biofilms were taken out after 7 and 14 days of immersion in different systems and were washed three times in PBS. The biofilms were stained under dark conditions for 15 min using a Live/Dead™ BacLight™ Bacterial Viability Kit (Thermo Fisher Scientific Inc., Waltham, MA, USA) before observation. The fluorescence of the biofilms was observed with a confocal laser scanning microscope (CLSM, ZEISS Microscopy GmbH, Jena, Germany). The thickness of the biofilm was measured in the 3D model.

2.5. Weight Loss Measurement

Before the pregrowth of biofilms, coupons were weighed and labeled. On the 7th and 14th days of incubation in different systems, the coupons were taken out for measurement. The coupons were immersed in Clark's solution (ASTM G1-03) and ultrasonically shaken for 20–40 s to remove corrosion products. The residual rust remover was washed away with distilled water and absolute ethanol, which were dried with N$_2$. The coupons with the removal of corrosion products were weighed with an electronic weighing scale. In each system, the weight loss of coupons was measured for three replicates.

2.6. Electrochemical Tests

The electrochemical corrosion behaviors of coupons were characterized by the Gamry 3000 electrochemical workstation (Garmy Instruments, Warminster, PA, USA). The EH40 steel coupon, platinum mesh, and Ag/AgCl (KCl-sat) electrodes served as working, counter, and reference electrodes, respectively, in the three-electrode system used in the tests. Linear polarization resistance (LPR) was measured after open circuit potential (OCP) became stabilized. The potential range was kept within ±10 mV versus OCP and the scan rate was set at 0.167 mV·s^{-1}. After 14 days of immersion, potentiodynamic polarization (PDP) curves were obtained at a potential sweep rate of 0.167 mV·s^{-1} in the range of −600 mV to +600 mV versus OCP.

2.7. Corrosion Morphology and Corrosion Product Characterizations

The coupons were taken out after 14 days of immersion in different systems. The corrosion products on the coupons were removed as described in Section 2.5. The surface morphology of the coupons was observed with a scanning electron microscope (SEM, Hitachi, Hitachi, Japan, TM3030). An XPS (Thermo Fisher Scientific Inc., Waltham, MA, USA,

ESCALAB 250Xi) was used to test the compositions of corrosion products. All peaks were adjusted using the C 1s peak (284.6 eV) and analyzed using XPS Peak (Version 4.1) software.

3. Results

3.1. Cell Counts and Biofilm Observation

Figure 1 shows sessile cell counts of *D. vulgaris* and *P. aeruginosa* after 7 and 14 days of incubation in different systems. In the full system without nitrate addition, the sessile cells of *D. vulgaris* were around 10^8 cfu·cm^{-2} on the 7th and 14th days. Meanwhile, in the starvation system without nitrate addition, the sessile cells of *D. vulgaris* decreased to ca. 10^5 cfu·cm^{-2} on the 7th and 14th days, suggesting that the growth of *D. vulgaris* was inhibited by the deficiency of the carbon source. The sessile cell numbers of *P. aeruginosa* were only about 10^4 cfu·cm^{-2} in the full system without nitrate addition on the 7th and 14th days. Similar to *D. vulgaris*, carbon source starvation reduced the sessile cell numbers of *P. aeruginosa* to below 10^2 cfu·cm^{-2} in the starvation system without nitrate addition on the 7th and 14th days. The sessile cell numbers of *P. aeruginosa* were three orders of magnitude lower than those of *D. vulgaris*, indicating that the growth of *P. aeruginosa* was inhibited by the deficiency of nitrate during 3 days of pregrowth and the next 14 days of incubation.
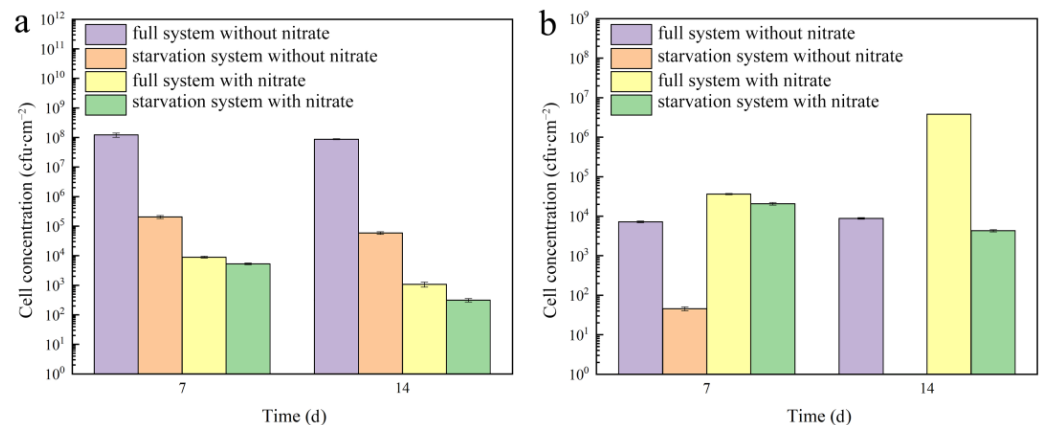

Figure 1. The sessile cell numbers of *D. vulgaris* (**a**) and *P. aeruginosa* (**b**) in different systems.

In the full system with nitrate addition, the sessile cell numbers of *D. vulgaris* were less than 10^4 cfu·cm^{-2} on the 7th and 14th days, indicating that the growth of *D. vulgaris* was greatly inhibited by nitrate. The inhibition of *D. vulgaris* was presumably caused by the competition of *P. aeruginosa* on organic carbon sources. Although carbon source starvation also decreased the sessile cell numbers of *D. vulgaris* in the presence of nitrate, the differences were smaller than one order of magnitude. Different from *D. vulgaris*, the growth of *P. aeruginosa* was promoted by nitrate, the sessile cell number of *P. aeruginosa* increased to more than 10^6 cfu·cm^{-2} in the full system with nitrate on the 14th day. Unexpectedly, the sessile cell numbers of *P. aeruginosa* maintained at about 10^4 cfu·cm^{-2} in the full system during the initial 7 days (the cell number of *P. aeruginosa* was also about 10^4 cfu·cm^{-2} after 3 days of pregrowth according to the previous study). The delay of growth was probably associated with the lag phase, during which *P. aeruginosa* adapted themselves to the new nitrate-sufficient environment to generate energy by nitrate respiration. *P. aeruginosa* became predominant in the full system with nitrate addition from the 7th day to the 14th day. The sessile cell number of *P. aeruginosa* was around three orders of magnitude higher than that of *D. vulgaris* on the 14th day. The inhibition of carbon source starvation on *P. aeruginosa* was slight on the 7th day, but rather strong on the 14th day with 10^6 versus 10^3 cfu·cm^{-2}. The decrease in sessile cell numbers of *D. vulgaris* and *P. aeruginosa* by carbon source starvation is in good accordance with the reports on single strains [23–25]. In addition, the absence or presence of nitrate was the determining factor of the dominant population, which might lead to different corrosion behaviors.

The CLSM images of biofilms on coupons exposed to different systems are shown in Figure 2. In the full system without nitrate addition, a high intensity of green fluorescence was observed on the 7th day, which is consistent with the 10^8 cfu·cm^{-2} sessile cell number of *D. vulgaris* in Figure 1. On the 14th day, the color of the biofilm changed to yellow, which resulted from the overlapped red fluorescence of increased dead cells and green fluorescence of living cells. The intensity of green fluorescence was much lower in the starvation system without nitrate addition, and that of red fluorescence was almost undetectable. Because *D. vulgaris* dominated the biofilm formed in the full system without nitrate addition (Figure 1), the green fluorescence mainly came from *D. vulgaris*. The introduction of nitrate into the full system resulted in thicker biofilm, which demonstrated that the total sessile cell number was decreased. Meanwhile, red fluorescence predominated on the 14th day, indicating that most cells were dead in the biofilm. The dead cells were supposed to be *D. vulgaris* killed by nitrite generated by *P. aeruginosa*. Carbon source starvation also led to lower fluorescence intensities in the presence of nitrate, but there were numerous dead cells, which is different from the case without nitrate addition.
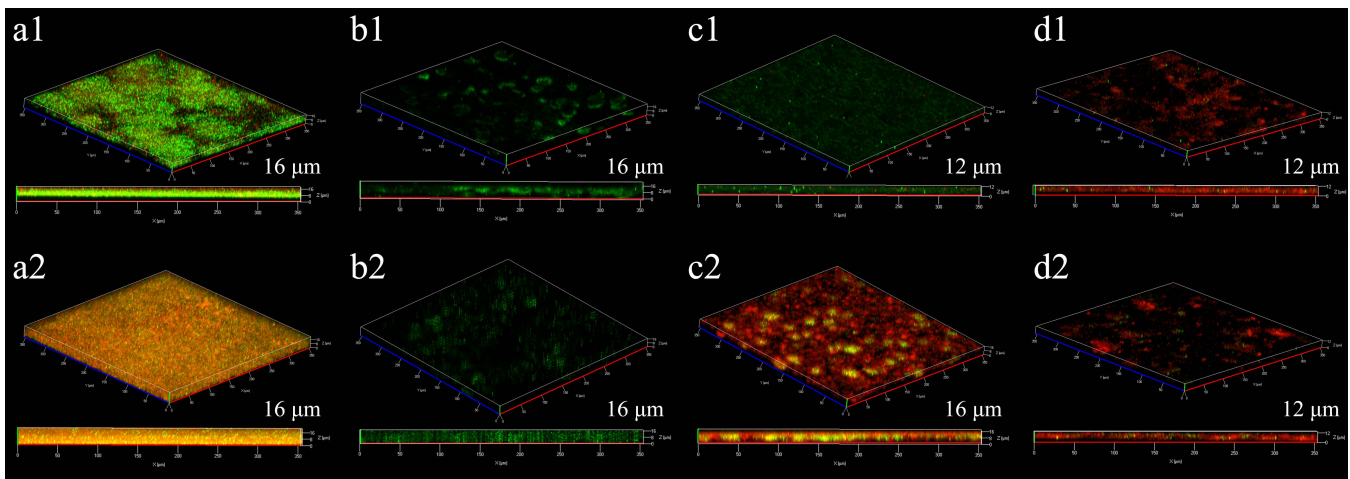

Figure 2. CLSM images of mixed biofilms on EH40 steel after 7 (**a1–d1**) and 14 days (**a2–d2**) of immersion in different systems: (**a1,a2**) full system without nitrate addition; (**b1,b2**) starvation system without nitrate addition; (**c1,c2**) full system with nitrate addition; and (**d1,d2**) starvation system with nitrate addition).

3.2. Nitrate/Sulfate Reduction Activity

The concentrations of NO$_3^-$, NO$_2^-$, SO$_4^{2-}$, and HS$^-$ ions in different systems before and after 14 days of incubation are shown in Table 1. Around 6.00 ppm, NO$_3^-$ was detected in the medium without NaNO$_3$ addition, which might originate from natural seawater. The consumption of SO$_4^{2-}$ and NO$_3^-$ in the full system without nitrate addition was 1728.4 and 5.2 ppm, respectively. The HS$^-$ accumulation was 66.75 ppm after 14 days of incubation. Carbon source starvation in systems without nitrate addition led to a decrease in SO$_4^{2-}$ consumption from 1728.4 to 1432.5 ppm and HS$^-$ accumulation from 66.8 to 55.2 ppm. The impact of carbon source starvation on ion utilization was closely related to the decrease in cell numbers and suggested weaker metabolic activity [26,27]. When nitrate was added, the consumption of NO$_3^-$ was around three times greater than that of SO$_4^{2-}$, accompanied by a decreased HS$^-$ content and a slight accumulation of 2 ppm NO$_2^-$. The consumption of NO$_3^-$ suggested the stimulation of *P. aeruginosa*. Meanwhile, the decreased consumption of SO$_4^{2-}$ suggested the inhibition of *D. vulgaris*. With the removal of carbon sources, SO$_4^{2-}$ and NO$_3^-$ consumption in systems with nitrate addition decreased from 847.3 to 477.3 ppm and from 2444.8 to 1681.7 ppm, respectively. The decreased utilization of electron acceptors demonstrated that both strains were inhibited under carbon source starvation. Moreover, the content of NO$_2^-$ in the starvation system with nitrate addition accumulated to 82.7 ppm, which was almost 40 times higher than that in the full system

with nitrate addition, indicating that the reduction in nitrate was incomplete owing to the starvation of electron donors.

Table 1. Concentrations of HS^-, SO_4^{2-}, NO_3^-, and NO_2^- before and after 14 days of incubation in different systems.

System	Full System without Nitrate Addition			Starvation System without Nitrate Addition			Full System with Nitrate Addition			Starvation System with Nitrate Addition		
ion concentration (ppm)	before	after	ΔC	before	after	ΔC	before	after	ΔC	before	after	ΔC
NO_2^-	—	—	—	—	—	—	—	2.1	+2.1	—	—	+82.7
NO_3^-	5.9	1.3	−4.6	6.0	0.8	−5.2	2652.7	207.9	−2444.8	2647.3	965.6	−1681.7
SO_4^{2-}	7534.2	5805.8	−1728.4	7534.2	6101.7	−1432.5	7537.0	6689.8	−847.3	7542.3	7065.0	−477.3
HS^-	—	66.8	+66.8	—	55.2	+55.2	—	33.9	+33.9	—	17.8	+17.8

3.3. Weight Loss and pH test

　　　Figures 3 and 4 depict the weight loss of coupons after 7 and 14 days of immersion in different systems. The background weight loss after 3 days of pregrowth was 0.13 mg·cm^{-2}, which is also marked with the dotted line in Figure 3. In the absence of nitrate, weight loss was increased by carbon source starvation from 0.19 to 0.43 mg·cm^{-2} and from 0.24 to 0.63 mg·cm^{-2} on the 7th and 14th days, respectively. The corrosion acceleration from carbon source starvation is in good accordance with previous reports in which enhanced EET was believed to be responsible for the promotion of MIC [6,7]. In the presence of nitrate, carbon source starvation led to an increase in weight loss from 0.29 to 0.65 mg·cm^{-2} on the 7th day, but a decrease from 1.98 to 1.05 mg·cm^{-2} on the 14th day. The results seem to be contradictory to the EET theory. Typically, carbon source starvation promotes MIC by forcing bacteria to extract electrons from metals, according to the EET theory. However, in systems with nitrate addition, starvation inhibited MIC in the last 7 days of incubation. The mechanism will be discussed below.
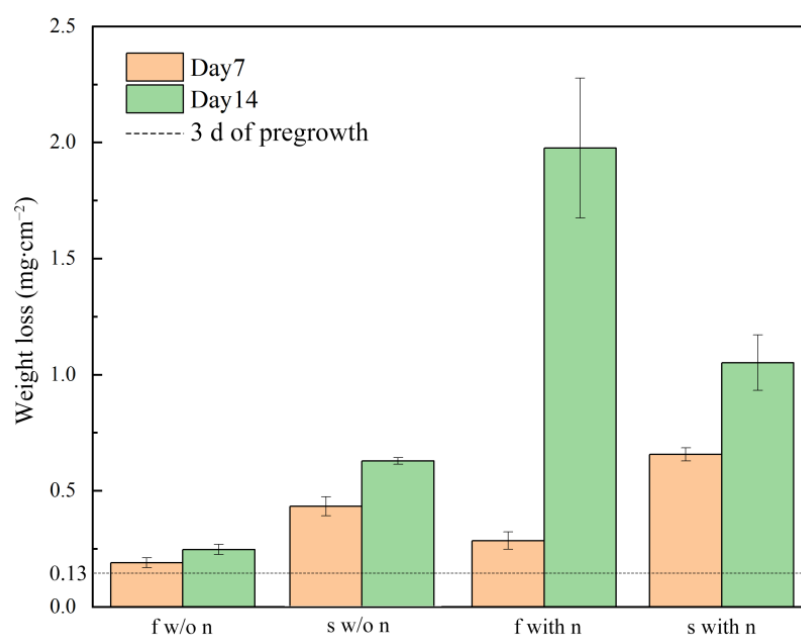

Figure 3. Corrosion weight loss of EH40 steel after 7 and 14 days of immersion in different systems (f w/o n: full system without nitrate addition, s w/o n: starvation system without nitrate addition, f with n: full system with nitrate addition, and s with n: starvation system with nitrate addition).
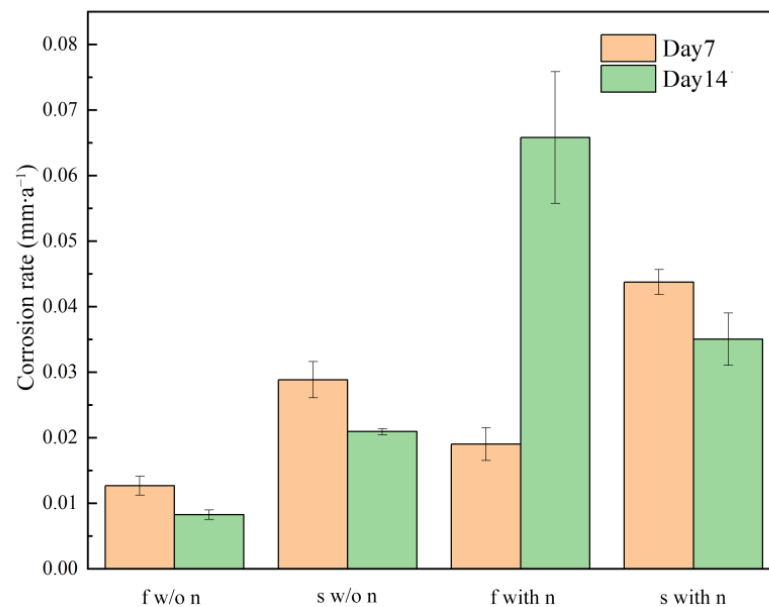
Figure 4. Corrosion rate of EH40 steel after 7 and 14 days of immersion in different systems (f w/o n: full system without nitrate addition, s w/o n: starvation system without nitrate addition, f with n: full system with nitrate addition, and s with n: starvation system with nitrate addition).

Figure 5 shows the pH values in different systems on the 14th day. The pH values in the full system without nitrate addition, the starvation system without nitrate addition, the full system with nitrate addition, and the starvation system with nitrate addition were 6.86, 6.77, 7.82, and 7.19, respectively. All pH values were close to 7, demonstrating that corrosion induced by the mixed cultures was not due to acids. The systems added with nitrate held higher values than those without addition. The increased pH values in systems with nitrate addition were closely related to OH^- generation during the reduction of nitrate to nitrite, nitrogen, or ammonia [26]. On the 14th day, the full system with nitrate addition held the highest weight loss, but also the highest pH, suggesting the highest nitrate reduction.
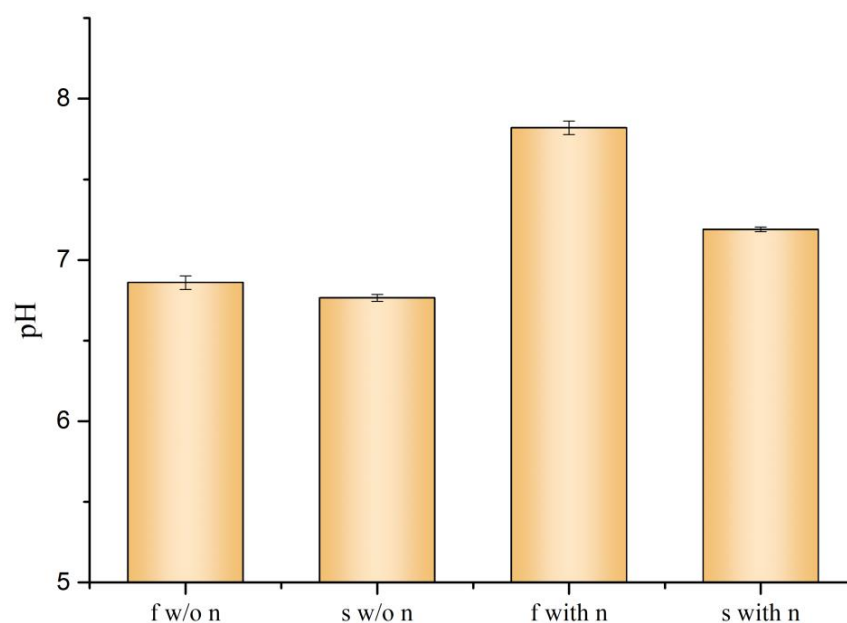

Figure 5. The pH values in different systems on the 14th day (f w/o n: full system without nitrate addition, s w/o n: starvation system without nitrate addition, f with n: full system with nitrate addition, and s with n: starvation system with nitrate addition).

3.4. Corrosion Morphology

Figure 6 displays SEM images of coupons with the removal of corrosion products after 14 days of immersion in different systems. Scratches formed during the sanding of coupons were observed on coupons immersed in systems without nitrate addition. No visible changes were induced by carbon source starvation in systems without nitrate addition. In the presence of nitrate, seldom were scratches on samples and the surface was accompanied by sporadic pits in the full system without nitrate addition. The severe corrosion is consistent with the highest weight loss in Figure 3. When carbon sources were removed in systems with nitrate addition, the surface of coupons became smoother and the scratches became weaker, indicating that corrosion was inhibited. However, corrosion in the starvation system with nitrate addition was still more severe than that in the starvation system without nitrate addition, which agrees with the results of weight loss. The corrosion caused by *D. vulgaris* in the present study was relatively weaker than other reported strains, and there might not have been significant pits [7]. *P. aeruginosa* caused pits were only observed in systems with nitrate addition, which is according to its metabolic activity.
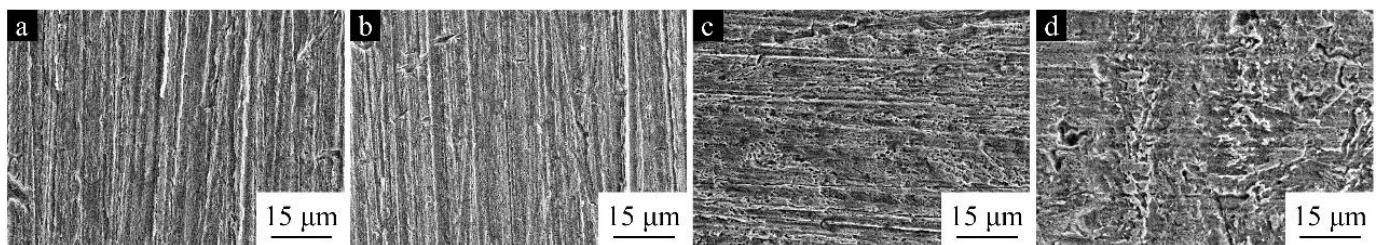

Figure 6. SEM images of EH40 steel with the removal of corrosion products after 14 days of immersion in different systems: (**a**) full system without nitrate addition; (**b**) starvation system without nitrate addition; (**c**) full system with nitrate addition; and (**d**) starvation system with nitrate addition.

3.5. Corrosion Product Compositions

After 14 days of incubation in different systems, the compositions of corrosion products were characterized by XPS, and are shown in Figure 7. The samples in different systems consisted of Fe^0, Fe_3O_4, FeO, FeS, and Fe_2O_3 with binding energies of 707.1, 708.2, 709.3, 710.3, and 711.4 eV, respectively [28–32]. The presence of FeS indicated that *D. vulgaris* participated in the corrosion of EH40 steel in all systems, which is in good accordance with the existence of *D. vulgaris* observed in cell counts.

The relative contents (RCs) of different components in corrosion products are exhibited in Table 2. In the full system without nitrate addition, metal Fe dominated with an RC of 41.5%, demonstrating fewer corrosion products and weak corrosion. When carbon source starvation was applied in systems without nitrate addition, the RC of metal Fe decreased to 38.4%, illustrating that corrosion was promoted. In the presence of nitrate, the RC of metal Fe in the full system was 31.7%, which was less than that of 34.9% in the starvation system. The result suggested that corrosion was inhibited under carbon starvation when nitrate was added. Meanwhile, the RCs of FeS in the full systems were higher than those in the starvation systems, which is closely related to the increased sulfate reduction activity of *D. vulgaris* with sufficient electron donors.
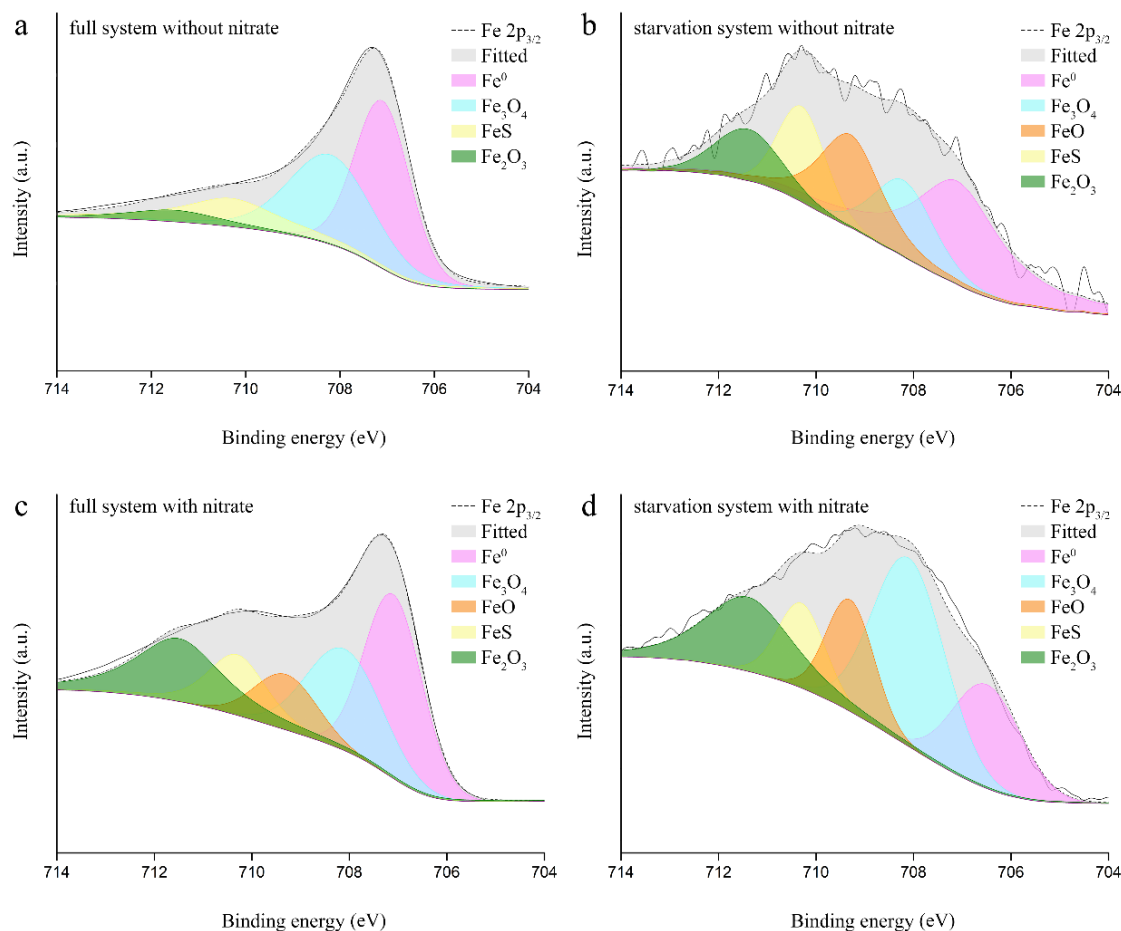
Figure 7. Fe 2p$_{3/2}$ spectra of corrosion products on EH40 steel after 14 days of immersion in different systems: (**a**) full system without nitrate addition; (**b**) starvation system without nitrate addition; (**c**) full system with nitrate addition; and (**d**) starvation system with nitrate addition.

Table 2. Relative contents of components in corrosion products of EH40 steel after 14 days of immersion in different systems.

Components of Corrosion Product	Positions (eV)	Full System without Nitrate Addition (at. %)	Starvation System without Nitrate Addition (at. %)	Full System with Nitrate Addition (at. %)	Starvation System with Nitrate Addition (at. %)
Fe^0	707.1	41.5	38.4	31.7	34.9
Fe$_3$O$_4$	708.2	35.4	15.4	23.0	17.1
FeO	709.3	0	21.0	10.4	19.6
FeS	710.3	17.2	14.0	12.6	10.9
Fe$_2$O$_3$	711.4	6.0	11.0	22.4	17.4

3.6. Electrochemical Characterizations

3.6.1. LPR Measurements

Figure 8 depicts the time-dependent polarization resistance (R_p) of coupons in different systems. All coupons exhibited similar R_p values at the initial 3 h of immersion, which demonstrated that all electrodes exhibited similar initial surface conditions. R_p recorded on coupons immersed in the full system without nitrate addition increased with time, demonstrating the reduction in the corrosion rate. This system held the highest R_p from the 1st day to the 14th day, which corresponds to the weakest corrosion. When carbon sources were removed in systems without nitrate addition, R_p decreased sharply in the first 3 days and then fluctuated around 80 KΩ·cm^2. The lower R_p values illustrated that

corrosion was promoted by carbon source starvation in the absence of nitrate. Different from the R_p in systems without nitrate addition, that in full systems with nitrate addition continuously decreased with time and became lower than that in the starvation system with nitrate addition after the 7th day. The R_p is in accordance with the unpredicted corrosion acceleration in the full system with nitrate addition. The impact of carbon source starvation on corrosion differed in systems with and without nitrate addition, which is believed to be closely related to the growth and metabolic activity of *D. vulgaris* and *P. aeruginosa* in the mixed cultures.
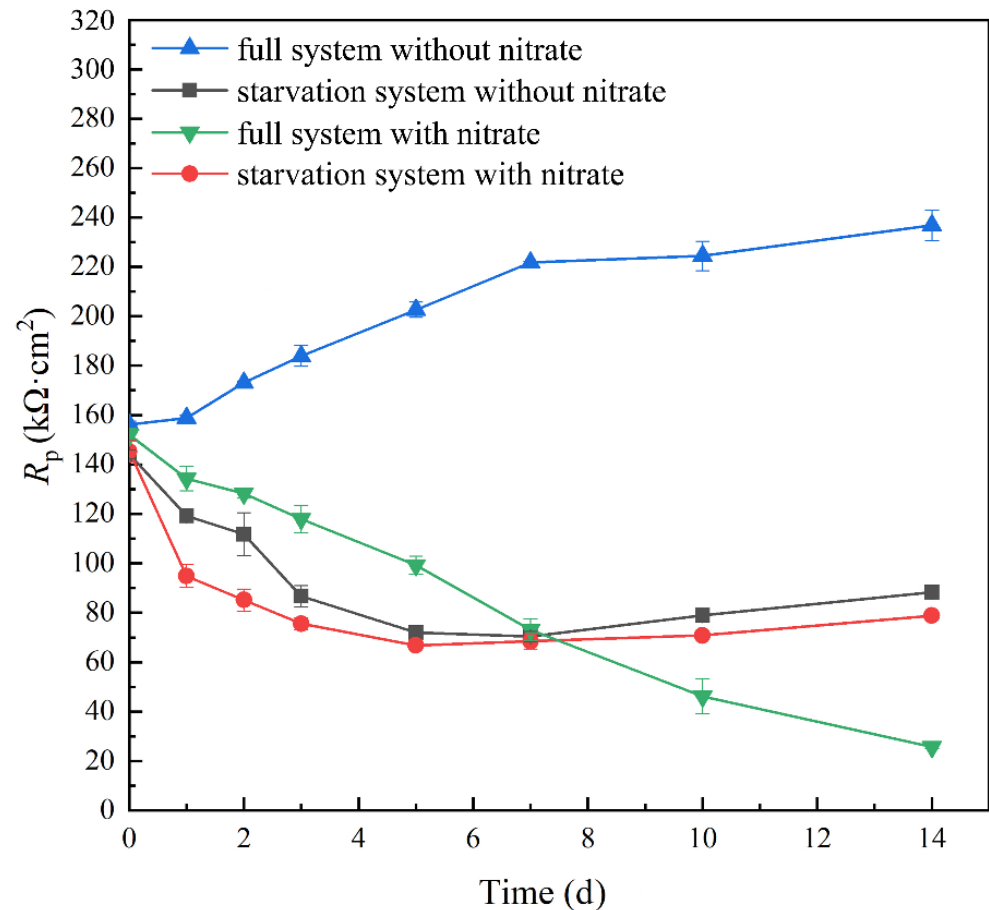

Figure 8. Time dependence of R_p in different systems.

3.6.2. PDP Curve Measurements

PDP curves of coupons immersed in different systems for 14 days are shown in Figure 9, and their fitting results are displayed in Table 3. The corrosion potential (E_{corr}) and cathodic branch of PDP curves were almost the same in full and starvation systems without nitration addition. However, the anodic branch held a larger current density in the starvation system, demonstrating that carbon source starvation stimulated the anodic electrochemical reaction, i.e., dissolution of Fe^0. Correspondingly, carbon source starvation increased the corrosion current density (i_{corr}) from 14.92 to 23.10 $\mu A \cdot cm^{-2}$ in systems without nitrate addition. Carbon source starvation in the presence of nitrate also resulted in a decrease in i_{corr} from 74.27 to 29.07 $\mu A \cdot cm^{-2}$, which is contradictory to the case without nitrate addition. Nitrate addition into the full system led to a negative shift of E_{corr} from −0.61 to −0.84 V and an increase in i_{corr} from 14.92 to 74.27 $\mu A \cdot cm^{-2}$, verifying the corrosion acceleration.
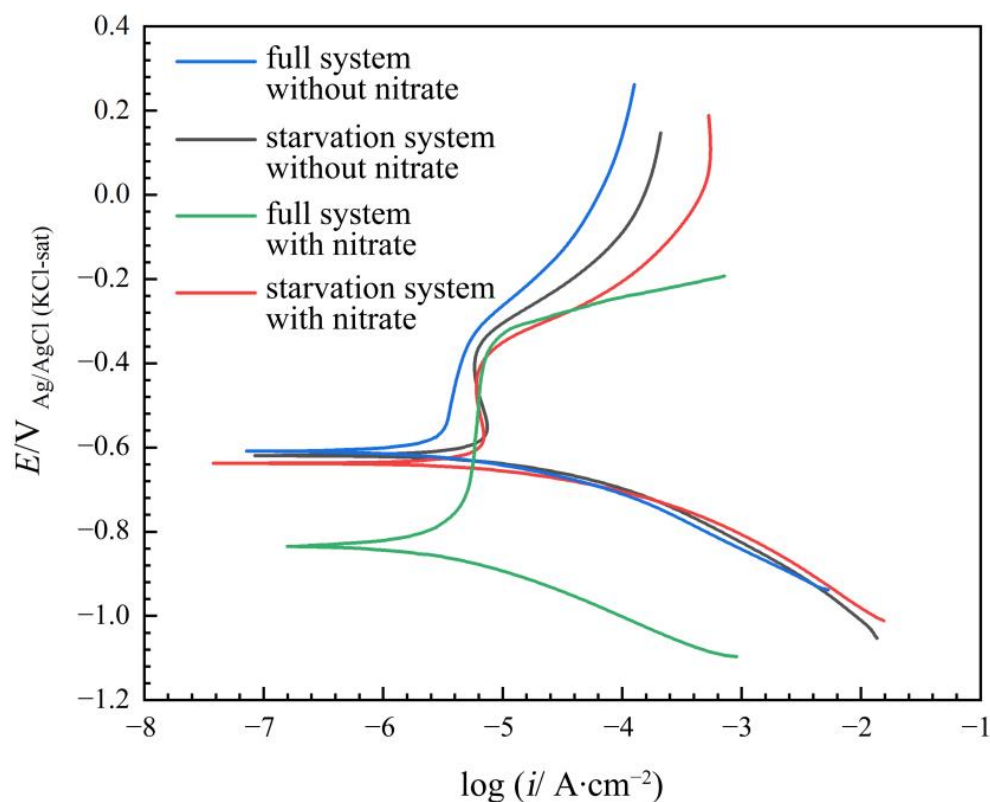
Figure 9. PDP curves on EH40 steel after 14 days of immersion in different systems.

Table 3. Electrochemical parameters derived from PDP curves.

Systems	E_{corr} (V $_{Ag/AgCl \, (KCl-sat)}$)	i_{corr} ($\mu A \cdot cm^{-2}$)
full system without nitrate addition	−0.61 ± 0.015	14.92 ± 1.12
starvation system without nitrate addition	−0.62 ± 0.024	23.10 ± 0.44
full system with nitrate addition	−0.84 ± 0.003	74.27 ± 0.031
starvation system with nitrate addition	−0.64 ± 0.013	29.07 ± 1.72

4. Discussion

The impact of carbon source starvation on the MIC of EH40 steel with the coexistence of *D. vulgaris* (SRB) and *P. aeruginosa* (NRB) was investigated in the present work. It was found that the impact of carbon source starvation varied with nitrate addition. In the absence of nitrate, carbon source starvation accelerated corrosion. However, in the presence of nitrate, carbon source starvation initially promoted corrosion but finally inhibited it. It is supposed that the differences in corrosion behavior are closely related to the cell numbers and physiological statuses of the strains.

In systems without nitrate addition, the cell numbers and metabolic activity of *P. aeruginosa* were limited owing to the shortage of electron acceptors. Although *P. aeruginosa* can promote EET mediated steel corrosion as a typical strain of NRB [33–35]. MIC caused by *P. aeruginosa* via EET is slight, as there are no adequate electron acceptors to achieve intracellular electron transfer. Furthermore, pH values suggested that acid-induced corrosion was also unrealistic. Therefore, in the absence of nitrate, MIC was mainly caused by *D. vulgaris* but not *P. aeruginosa*. After the pregrowth and incubation in media without nitrate addition, the dormant cells of *P. aeruginosa* were supposed to maintain lower metabolic activity than *D. vulgaris*. Moreover, the cell numbers of *P. aeruginosa* were also three orders of magnitude lower than those of *D. vulgaris*. Taken together, it was supposed that the cells of *P. aeruginosa* had almost no influence on the effect of carbon source starvation on *D. vulgaris*. Considering that the cells of *P. aeruginosa* have almost no influence on MIC and carbon source competition, the effect of carbon source starvation on corrosion is in good

accordance with previous studies in which starvation was applied to the pure culture of
D. vulgaris [7]. When carbon sources were removed, the number of *D. vulgaris* in biofilms
of mixed cultures was around 10^5 cfu·cm^{-2}, which was about three orders of magnitude
lower than that in the full system. However, the biofilm with less sessile cell numbers
resulted in a higher corrosion rate. It has been widely demonstrated that species from the
genus *Desulfovibrio* can switch from organic electron donors to Fe^0 as the electron donor
to accelerate corrosion when carbon sources were limited [36,37], and the cells harvesting
electrons from Fe^0 in biofilms determine the corrosion rate [38]. Although the starvation
system held lower *D. vulgaris* cells in biofilms than that in the full system, the proportion
of cells that obtain electrons from Fe^0 for respiration was far higher than that with rich
organic carbon, leading to a higher corrosion rate.

In systems with nitrate addition, both *D. vulgaris* and *P. aeruginosa* had the potential to
induce MIC as there was enough sulfate and nitrate for the anaerobic respiration. In systems
with nitrate addition, the impact of carbon source starvation on *D. vulgaris* caused corrosion
was difficult to speculate. However, the corrosion caused by *D. vulgaris* could be evaluated
by physiological results and theories. In *D. vulgaris*, nitrate works as a stress signal to initiate
the nitrite stress response, which is generated by nitrate reduction [27]. The growth and
energy metabolism activities of *D. vulgaris* were inhibited in response to nitrite stress [39].
It was reported that 50 mM nitrate is enough to inhibit the pure culture of *D. vulgaris*,
while the nitrate concentration used in the present work is 59 mM [27]. Besides nitrate,
nitrite generated from the nitrate reduction of *P. aeruginosa* is exported to extracellular
space. The direct response to nitrate is more severe than nitrate, and the oxidative damage
of nitrite is deadly to *D. vulgaris* [39]. In *D. vulgaris*, the response to nitrate and nitrite
downregulates genes for sulfate reduction and inhibits growth, resulting in a status similar
to that of *P. aeruginosa* in systems without nitrate addition. As observed in cell counts
and CLSM, the growth of *D. vulgaris* is inhibited. The sessile cell numbers were kept at a
relatively low concentration of less than 10^4 cfu·cm^{-2}, reaching the threshold below which
the MIC is inhibited by growth inhibition [7]. Taken together, the cell numbers and sulfate
reduction activity of *D. vulgaris* were lower than that in the full system without nitrate
addition. Therefore, MIC induced by *D. vulgaris* in systems without nitrate addition was
below 0.012 mm·a^{-1}. Compared with the corrosion rate in systems with nitrate addition,
P. aeruginosa was the main factor of MIC. Besides, 82.7 ppm of nitrite was accumulated in
the starvation system with nitrate addition on the 14th day. Nitrite with a concentration of
50 ppm and 100 ppm was reported to cause corrosion of carbon steel [40]. In the present
work, the effect of nitrite and *D. vulgaris* together proved the conclusion that starvation
inhibited MIC of *P. aeruginosa* in the last 7 days. In the full system, *P. aeruginosa* grew rapidly
from ca.10^4 cfu·cm^{-2} on the 7th day to 10^6 cfu·cm^{-2} on the 14th day. However, the sessile
cells of *P. aeruginosa* maintained at ca.10^4 cfu·cm^{-2} before the 7th day. It seems that the
acceleration of the corrosion rate has a relation with the cell numbers of *P. aeruginosa*. The
possible mechanism: the organic electron donors were consumed to provide starvation
conditions at the bottom of the biofilm and accelerate corrosion, and the accumulation of
sessile cells stimulated the EET activity of *P. aeruginosa*. The specific electron shuttle of
P. aeruginosa, phenazine, was reported to be synthesized and secreted when cell numbers
reach a high level [41]. That would also explain why *D. vulgaris* had a dissimilar population
effect under starvation in systems without nitrate addition, as there is no phenazine or
related regulation system in *D. vulgaris*.

5. Conclusions

This work investigated the impact of carbon source starvation on EH40 steel induced
by mixed cultures in media without and with nitrate addition, and it was found that nitrate
played a decisive role in corrosion impact. *D. vulgaris* dominated in biofilms when nitrate
was not added, and the corrosion rate doubled with starvation as a result of its improved
EET capacity. Meanwhile, corrosion was mainly affected by *P. aeruginosa* with the addition

of nitrate, and an amount of sessile cells three orders of magnitude lower as a result of starvation on day 14 led to half the corrosion rate.

This work implies the significant role of EET capacity and sessile cell quantity in MIC of mixed cultures, and the expression of genes related to EET and biofilms of different strains will be considered to allow a deeper understanding of mechanisms in the complex systems.

References

1. Gaines, R.H. Bacterial Activity as a Corrosive Influence in the Soil. *Ind. Eng. Chem.* **1910**, *2*, 128–130. [CrossRef]
2. Garrett, J.H. *The Action of Water on Lead*; HK Lewis: London, UK, 1891.
3. Lekbach, Y.; Liu, T.; Li, Y.; Moradi, M.; Dou, W.; Xu, D.; Smith, J.A.; Lovley, D.R. Microbial corrosion of metals: The corrosion microbiome. *Adv. Microb. Physiol.* **2021**, *78*, 317–390.
4. Holmes, D.E.; Tang, H.; Woodard, T.; Liang, D.; Zhou, J.; Liu, X.; Lovley, D.R. Cytochrome-mediated direct electron uptake from metallic iron by *Methanosarcina acetivorans*. *mLife* **2022**, *1*, 443–447. [CrossRef]
5. Tang, H.; Holmes, D.E.; Ueki, T.; Palacios, P.A.; Lovley, D.R. Iron corrosion via direct metal-microbe electron transfer. *mBio* **2019**, *10*, e00303-19. [CrossRef]
6. Gu, T.; Jia, R.; Unsal, T.; Xu, D. Toward a better understanding of microbiologically influenced corrosion caused by sulfate reducing bacteria. *J. Mater. Sci. Technol.* **2019**, *35*, 631–636. [CrossRef]
7. Xu, D.; Gu, T. Carbon source starvation triggered more aggressive corrosion against carbon steel by the *Desulfovibrio vulgaris* biofilm. *Int. Biodeterior. Biodegrad.* **2014**, *91*, 74–81. [CrossRef]
8. Jia, R.; Yang, D.; Xu, J.; Xu, D.; Gu, T. Microbiologically influenced corrosion of C1018 carbon steel by nitrate reducing *Pseudomonas aeruginosa* biofilm under organic carbon starvation. *Corros. Sci.* **2017**, *127*, 1–9. [CrossRef]
9. Qian, H.; Zhang, D.; Lou, Y.; Li, Z.; Xu, D.; Du, C.; Li, X. Laboratory investigation of microbiologically influenced corrosion of Q235 carbon steel by halophilic archaea *Natronorubrum tibetense*. *Corros. Sci.* **2018**, *145*, 151–161. [CrossRef]
10. Rajala, P.; Cheng, D.Q.; Rice, S.A. Sulfate-dependant microbially induced corrosion of mild steel in the deep sea: A 10-year microbiome study. *Microbiome* **2022**, *10*, 4. [CrossRef]
11. Schwermer, C.U.; Lavik, G.; Abed, R.M.M.; Dunsmore, B.; Ferdelman, T.G.; Stoodley, P.; Gieseke, A. Impact of nitrate on the structure and function of bacterial biofilm communities in pipelines used for injection of seawater into oil fields. *Appl. Environ. Microbiol.* **2008**, *74*, 2841–2851. [CrossRef]
12. Lai, R.; Li, Q.; Cheng, C.; Shen, H.; Liu, S.; Luo, Y.; Zhang, Z.; Sun, S. Bio-competitive exclusion of sulfate-reducing bacteria and its anticorrosion property. *J. Pet. Sci. Eng.* **2020**, *194*, 107480. [CrossRef]
13. Kebbouche-Gana, S.; Gana, M.L. Biocorrosion of carbon steel by a nitrate-utilizing consortium of sulfate-reducing bacteria obtained from an Algerian oil field. *Ann. Microbiol.* **2012**, *62*, 203–210. [CrossRef]
14. Chen, H.; Wang, W.; Du, C.; Wang, X.; Zhang, X. Study on the microbiological corrosion in oilfield reinjection water system inhibited by biological competition technology. *Ind. Water Treat.* **2013**, *33*, 79–81.
15. Nemati, M.; Jenneman, G.E.; Voordouw, G. Impact of nitrate-mediated microbial control of souring in oil reservoirs on the extent of corrosion. *Biotechnol. Progress* **2001**, *17*, 852–859. [CrossRef]
16. Hubert, C.; Nemati, M.; Jenneman, G. Corrosion risk associated with microbial souring control using nitrate or nitrite. *Appl. Microbiol. Biotechnol.* **2005**, *68*, 272–282. [CrossRef]
17. Fu, Q.; Xu, J.; Wei, B.; Qin, Q.; Bai, Y.; Yu, C.; Sun, C. Biologically competitive effect of *Desulfovibrio desulfurican* and *Pseudomonas stutzeri* on corrosion of X80 pipeline steel in the Shenyang soil solution. *Bioelectrochemistry* **2022**, *145*, 108051. [CrossRef]
18. Carlson, H.K.; Kuehl, J.V.; Hazra, A.B.; Justice, N.B.; Stoeva, M.K.; Sczesnak, A.; Mullan, M.R.; Iavarone, A.T.; Engelbrektson, A.; Price, M.N.; et al. Mechanisms of direct inhibition of the respiratory sulfate-reduction pathway by (per) chlorate and nitrate. *ISME J.* **2015**, *9*, 1295–1305. [CrossRef]

19. Farley, J.R.; Cryns, D.F.; Yang, Y.; Segel, I.H. Adenosine triphosphate sulfurylase from penicillium chrysogenum. Steady state kinetics of the forward and reverse reactions. *J. Biol. Chem.* **1976**, *251*, 4389–4397. [CrossRef]

20. O'Reilly, C.; Colleran, E. Toxicity of nitrite toward mesophilic and thermophilic sulphate-reducing, methanogenic and syntrophic populations in anaerobic sludge. *J. Ind. Microbiol. Biotechnol.* **2005**, *32*, 46–52. [CrossRef]

21. Sun, Z.; Wu, J.; Zhang, D.; Li, C.; Zhu, L.; Li, E. Influence of nitrate concentrations on EH40 steel corrosion affected by coexistence of *Desulfovibrio desulfuricans* and *Pseudomonas aeruginosa* bacteria. *J. Oceanol. Limnol.* **2022**, *1*, 14. [CrossRef]

22. Chen, J.; Wu, J.; Wang, P.; Zhang, D.; Chen, S.; Tan, F. Corrosion of 907 steel influenced by sulfate-reducing bacteria. *J. Mater. Eng. Perform.* **2019**, *28*, 1469–1479. [CrossRef]

23. Nguyen, D.; Joshi-Datar, A.; Lepine, F.; Bauerle, E.; Olakanmi, O.; Beer, K.; Mckay, G.; Siehnel, R.; Schafhauser, J.; Wang, Y.; et al. Active starvation responses mediate antibiotic tolerance in biofilms and nutrient-limited bacteria. *Science* **2011**, *334*, 982–986. [CrossRef]

24. Heise, S.; Reichardt, W. Anaerobic starvation survival of marine bacteria. *Kiel. Meeresforsch.-Sonderh.* **1991**, *8*, 97–101.

25. Li, E.; Wu, J.; Zhang, D.; Wang, P.; Wang, Y.; Xu, M.; Li, C.; Sun, Z.; Zhu, L. Electron donor dependent inhibition mechanisms of D-phenylalanine on corrosion of Q235 carbon steel caused by *Desulfovibrio* sp. Huiquan2017. *Corros. Sci.* **2021**, *188*, 109493. [CrossRef]

26. Greene, E.A.; Hubert, C.; Nemati, M.; Jenneman, G.E.; Voordouw, G. Nitrite reductase activity of sulphate-reducing bacteria prevents their inhibition by nitrate-reducing, sulphide-oxidizing bacteria. *Environ. Microbiol.* **2003**, *5*, 607–617. [CrossRef]

27. He, Q.; He, Z.; Joyner, D.C.; Joachimiak, M.; Price, M.N.; Yang, Z.K.; Yen, H.B.; Hemme, C.L.; Chen, W.; Fields, M.M.; et al. Impact of elevated nitrate on sulfate-reducing bacteria: A comparative study of *Desulfovibrio vulgaris*. *ISME J.* **2010**, *4*, 1386–1397. [CrossRef]

28. Li, Y.; Feng, S.; Liu, H.; Tian, X.; Xia, Y.; Li, M.; Xu, K.; Yu, H.; Liu, Q.; Chen, C. Bacterial distribution in SRB biofilm affects MIC pitting of carbon steel studied using FIB-SEM. *Corros. Sci.* **2020**, *167*, 108512. [CrossRef]

29. Allen, G.C.; Curtis, M.T.; Hooper, A.J.; Tucker, P.M. X-Ray photoelectron spectroscopy of iron–oxygen systems. *J. Chem. Soc. Dalton Trans.* **1974**, *14*, 1525–1530. [CrossRef]

30. Best, S.A.; Brant, P.; Feltham, R.D.; Rauchfuss, T.B.; Roundhill, D.M.; Walton, R.A. X-ray photoelectron spectra of inorganic molecules. 18. Observations on sulfur 2p binding energies in transition metal complexes of sulfur-containing ligands. *Inorg. Chem.* **1977**, *16*, 1976–1979. [CrossRef]

31. Hawn, D.D.; DeKoven, B.M. Deconvolution as a correction for photoelectron inelastic energy losses in the core level XPS spectra of iron oxides. *Surf. Interface Anal.* **1987**, *10*, 63–74. [CrossRef]

32. Cui, L.; Liu, Z.; Xu, D.; Hu, P.; Shao, J.; Du, C.; Li, X. The study of microbiologically influenced corrosion of 2205 duplex stainless steel based on high-resolution characterization. *Corros. Sci.* **2020**, *174*, 108842. [CrossRef]

33. Zhou, E.; Zhang, M.; Huang, Y.; Li, H.; Wang, J.; Jiang, G. Accelerated biocorrosion of stainless steel in marine water via extracellular electron transfer encoding gene *phzH* of *Pseudomonas aeruginosa*. *Water Res.* **2022**, *220*, 118634. [CrossRef]

34. Jia, R.; Yang, D.; Xu, D.; Gu, T. Electron transfer mediators accelerated the microbiologically influence corrosion against carbon steel by nitrate reducing *Pseudomonas aeruginosa* biofilm. *Bioelectrochemistry* **2017**, *118*, 38–46. [CrossRef]

35. Huang, L.; Huang, Y.; Lou, Y.; Qian, H.; Xu, D.; Ma, L.; Jiang, C. Pyocyanin-modifying genes *phzM* and *phzS* regulated the extracellular electron transfer in microbiologically-influenced corrosion of X80 carbon steel by *Pseudomonas aeruginosa*. *Corros. Sci.* **2020**, *164*, 108355. [CrossRef]

36. Ueki, T.; Lovley, D.R. *Desulfovibrio vulgaris* as a model microbe for the study of corrosion under sulfate-reducing conditions. *mLife* **2022**, *1*, 13–20. [CrossRef]

37. Dou, W.; Liu, J.; Cai, W.; Wang, D.; Jia, R.; Chen, S.; Gu, T. Electrochemical investigation of increased carbon steel corrosion via extracellular electron transfer by a sulfate reducing bacterium under carbon source starvation. *Corros. Sci.* **2019**, *150*, 258–267. [CrossRef]

38. McCully, A.L.; Spormann, A.M. Direct cathodic electron uptake coupled to sulfate reduction by *Desulfovibrio ferrophilus* IS5 biofilms. *Environ. Microbiol.* **2020**, *22*, 4794–4807. [CrossRef]

39. Haveman, S.A.; Greene, E.A.; Stilwell, C.P.; Voordouw, C.P.; Voordouw, G. Physiological and gene expression analysis of inhibition of *Desulfovibrio vulgaris* Hildenborough by nitrite. *J. Bacteriol.* **2004**, *186*, 7944–7950. [CrossRef]

40. Lee, D.Y.; Kim, W.C.; Kim, J.G. Effect of nitrite concentration on the corrosion behaviour of carbon steel pipelines in synthetic tap water. *Corros. Sci.* **2012**, *64*, 105–114. [CrossRef]

41. Higgins, S.; Heeb, S.; Rampioni, G.; Fletcher, M.P.; Williams, P.; Cámara, M. Differential regulation of the phenazine biosynthetic operons by quorum sensing in *Pseudomonas aeruginosa* PAO1-N. *Front. Cell. Infect. Microbiol.* **2018**, *8*, 252. [CrossRef]